JCBFM

Targeting Na,K-ATPase-Src signaling to normalize cerebral blood flow in a murine model of familial hemiplegic migraine

Christian Staehr[1,2,3] [iD], Halvor Østerby Guldbrandsen[1],
Casper Homilius[1], Laura Øllegaard Johnsen[1], Dmitry Postnov[4],
Tina M Pedersen[1] [iD], Sandrine Pierre[5], Shaun L Sandow[3,6] and
Vladimir V Matchkov[1] [iD]

Abstract

Familial hemiplegic migraine type 2 (FHM2) is linked to Na,K-ATPase α_2 isoform mutations, including that of G301R. Mice heterozygous for this mutation ($\alpha_2^{+/G301R}$) show cerebrovascular hypercontractility associated with amplified Src kinase signaling, and exaggerated neurovascular coupling. This study hypothesized that targeting Na,K-ATPase-dependent Src phosphorylation with pNaKtide would normalize cerebral perfusion and neurovascular coupling in $\alpha_2^{+/G301R}$ mice. The effect of pNaKtide on cerebral blood flow and neurovascular coupling was assessed using laser speckle contrast imaging in awake, head-fixed mice with cranial windows in a longitudinal study design. At baseline, compared to wild type, $\alpha_2^{+/G301R}$ mice exhibited increased middle cerebral artery tone; with whisker stimulation leading to an exaggerated increase in sensory cortex blood flow. No difference between genotypes in telemetrically assessed blood pressure occurred. The exaggerated neurovascular coupling in $\alpha_2^{+/G301R}$ mice was associated with increased $K_{ir}2.1$ channel expression in cerebrovascular endothelium. Two weeks pNaKtide treatment normalized cerebral artery tone, endothelial $K_{ir}2.1$ expression, and neurovascular coupling in $\alpha_2^{+/G301R}$ mice. Inhibition of the Na,K-ATPase-dependent Src kinase signaling with pNaKtide prevented excessive vasoconstriction and disturbances in neurovascular coupling in $\alpha_2^{+/G301R}$ mice. pNaKtide had only minor hypotensive effect similar in both genotypes. These results demonstrate a novel treatment target to normalize cerebral perfusion in FHM2.

Introduction

Familial hemiplegic migraine type 2 (FHM2) is associated with mutations in the *ATP1A2* gene encoding the α_2 Na,K-ATPase isoform.[1–3] The Na,K-ATPase is an ion pump that clears K^+ and establishes the transmembrane Na^+ gradient.[4] This gradient is, among many other functions, used by glutamate transporters to transfer glutamate into astrocytes.[5] The α_2 isoform of the *ATP1A2* gene is expressed in glial and vascular cells,[6,7] but not in mature neurons,[8] suggesting that the pathophysiology of FHM2 may not directly originate from neuronal cells.[9] Currently, over 180 different FHM2-associated *ATP1A2* mutations have been

[1]Department of Biomedicine, Aarhus University, Aarhus, Denmark
[2]Department of Anesthesiology and Intensive Care, Aarhus University Hospital, Aarhus, Denmark
[3]School of Clinical Medicine, University of Queensland, St Lucia, Qld, Australia
[4]Center of Functionally Integrative Neuroscience, Aarhus University, Aarhus, Denmark
[5]Institute for Interdisciplinary Research, Marshall University, Huntington, USA
[6]School of Health, University of the Sunshine Coast, Maroochydore, Qld, Australia

Corresponding author:
Christian Staehr, Høegh-Guldbergs Gade 10, 8000 Aarhus, Denmark.
Email: chst@biomed.au.dk

identified. One of these is the G301R mutation, which is associated with a severe FHM2 phenotype that in some cases includes episodes of protracted coma in migraine attacks, seizures, and cerebellar signs.[10] Mice heterozygous for this mutation, $\alpha_2^{+/G301R}$ mice, show impaired astrocytic glutamate uptake *in vitro*.[11] *In vivo* and *in vitro* data from another heterozygous FHM2 model, $\alpha_2^{+/R887}$ mice, also show impaired astrocytic glutamate uptake.[12–14] A suppression of the Na, K-ATPase activity may reduce clearance of interstitial K^+ released during neuronal activity,[4] as it is observed in $\alpha_2^{+/R887}$ mice.[14] This is, however, controversial, as the study on brain slices from $\alpha_2^{+/G301R}$ and wild type mice did not report any difference in clearance of K^+ elevated upon neuronal activity, and suggested that heterozygosity for this FHM2-associated *ATP1A2* mutation is not sufficient for significant suppression of the Na, K-ATPase activity.[15] This contrasts with a previous report suggesting impaired glutamate uptake in $\alpha_2^{+/G301R}$ brains *in vitro*.[11] Migraine aura is caused by a spreading wave of cortical depolarization, as cortical spreading depression (CSD). Importantly, elevated glutamate and K^+ concentrations in the brain parenchyma are proposed to increase susceptibility to CSD.[16,17] Accordingly, reduced clearance of K^+ and glutamate during neuronal activity in mouse models of FHM2, including $\alpha_2^{+/G301R}$ mice, might explain their increased susceptibility to CSD.[12–14,18]

The increased cerebral artery constriction in $\alpha_2^{+/G301R}$ mice is associated with an elevated sensitivity to changes in intracellular Ca^{2+} in the contractile machinery of vascular smooth muscle cells.[19] In mouse middle cerebral arteries, sensitivity to intracellular Ca^{2+} in vascular smooth muscle cells may be increased by Na,K-ATPase-dependent Src kinase signaling.[9,19] Accordingly, cerebral arteries of the $\alpha_2^{+/G301R}$ mice show augmented signaling in the Src kinase pathway.[19] Notably, the $\alpha_2^{+/G301R}$ mice have exaggerated neurovascular coupling (NVC); as an elevated local hyperemic response to neuronal activity in the brain.[20] Similar abnormalities occur in migraine with aura, although the underlying mechanism/s remains elusive.[21,22] Cerebrovascular endothelial $K_{ir}2.1$ ion channels are suggested to play a key role in NVC.[23–27] Thus, the increased concentration of extracellular K^+ occurring upon neuronal excitation is detected by the capillary endothelium.[27] The neurovascular signal may subsequently be transmitted upstream to the arterioles via the endothelium in a $K_{ir}2.1$-dependent manner, resulting in arteriole dilation.[23,24,28] Consistent with this hypothesis, the exaggerated NVC in $\alpha_2^{+/G301R}$ mice is attributed to increased cerebral artery endothelial $K_{ir}2.1$ channel expression.[20] The microvascular endothelial importance for this neurovascular defect in $\alpha_2^{+/G301R}$

mice was further validated in *ex vivo* brain slice preparations and isolated middle cerebral arteries.[20]

This study determined the potential for chronic inhibition of the Na,K-ATPase-dependent Src kinase pathway as a therapeutic strategy to ameliorate cerebral blood flow disturbance in FHM2 patients, using the $\alpha_2^{+/G301R}$ mouse as a model of this disorder. Specifically, it was hypothesized that chronic treatment with pNaKtide,[29–33] a peptide mimicking the inhibitory Src-binding domain of the Na,K-ATPase,[34] would restore normal cerebral hemodynamics in these mice. To test this hypothesis, $\alpha_2^{+/G301R}$ and matched wild type (WT) mice were chronically treated with pNaKtide. Arterial blood pressure, blood electrolytes, cerebral blood flow and NVC were assessed in awake mice at baseline and after 14 days of treatment.

Methods

Animal experiments

The Animal Experiments Inspectorate of the Danish Ministry of Environment and Food granted approval for the study (#2019-15-0201-00341, C2 and #2021-15-0201-01074). All procedures were performed according to the guidelines from Directive 2010/63/EU of the European Parliament on the protection of animals used for scientific purposes. Animal experiments were reported in accordance with the ARRIVE (Animal Research: Reporting *in vivo* Experiments) guidelines. The breeding and genotyping of C57BL/6jRj mice heterozygous for the G301R knock-in mutation in the *Atp1a2* gene has previously been described.[11,19] The studies were performed using $\alpha_2^{+/G301R}$ and WT littermate mice obtained by crossing $\alpha_2^{+/G301R}$ mice with C57BL/6jRj mice (Janvier Labs, Le Genest-Saint-Isle, France). Sample size was based on previous studies on $\alpha_2^{+/G301R}$ mice.[19,20] Study mice were 3–4 months old and kept on a 12:12 light/dark cycle with *ad libitum* access to food and water. The study focus was on female mice, noting that human females have a higher incidence of migraine over males, and female mice were calm during head fixation for whisker stimulation, whereas male mice tended to gnaw whiskers of littermates. Notably, the cerebrovascular phenotype in $\alpha_2^{+/G301R}$ mice was previously reported to be similar between sexes.[20]

The pNaKtide peptide (25 mg/kg, diluted in sterile 0.9% NaCl at concentration 6.25 mg/ml)[34] was injected intraperitoneally every second day for 14 days. A control group was treated with an equivalent volume of 0.9% NaCl as vehicle. An equal number of mice were randomized to receive either pNaKtide or saline. The study was performed in a blinded fashion, i.e., researchers doing experiments and scans were blinded

to genotype and treatment groups. None of the mice exhibited symptoms of discomfort or pain.

Chronic cranial window preparation

Mice were anesthetized with ketamine (33 mg/100 g; Ketaminol vet, Intervet International, Netherlands) and xylazine (7.5 mg/100 g; Narcoxyl vet, Intervet International). A maintenance dose (25% of initial vol.) was injected every 45 min. The skin and periosteum were removed, and a bilateral steel head bar was attached to the bone with resin-based dentaladhesiveresin (Heliobond, Ivoclar, Liechtenstein) and glue (Loctite 401, Henkel, Denmark). A round craniotomy with a diameter of 4 mm was drilled and a round glass window that fitted the cranial opening was glued to the bone. The dura was left intact. The mice received postsurgical analgesics by subcutaneous injections of 0.1 mg/kg buprenorphine four times daily for two days. Additionally, buprenorphine was supplemented to drinking water (0.01 mg/mL) for three days after surgery. Mice were allowed to recover from the surgery for at least 2 wks. The mice were trained to be headfixed over 6–8 training sessions. The training sessions took place every second day starting with a duration of 5 min and ending at 45 min. After each training session, the mouse was rewarded with condensed milk.

Laser speckle contrast imaging

To deliver coherent light to the sample, side illumination with volume holographic grating stabilized laser diode[35] (785 nm, LDM785, Thorlabs, USA) controlled by current and temperature controller (CLD1010LP, Thorlabs) was used. Backscattered light was collected with a lens (VZM200i, Edmund Optics, USA) at $1\times$ magnification and recorded with a CMOS camera (acA2000, Basler, Germany). A linear polarizer was fitted in front of the objective and adjusted to minimize reflections and reduce the number of recorded single scattering events.[36] The speckle size was maintained with an iris and set to approximately 2.5 pixels. The field of view was 1024×1024 pixels, and a frame rate of 50 frames per sec was used to assess NVC. In a subset of recordings where single vessel diameter and flow were assessed in awake mice, 194 frames per sec were recorded in a 512×512 pixels field-of-view.

To characterize the blurring of speckle pattern, temporal contrast analysis was performed. Namely, the contrast (K) for every pixel was calculated; $K = \frac{\sigma}{\langle I \rangle}$, where σ is the standard deviation and $\langle I \rangle$ is the mean intensity across 25 consecutive frames. The contrast value has a complex relation to actual blood flow,[37] which depends on system parameters and an appropriate light scattering model. In this study, a simplified

model was used, which allows calculation of quantitative blood flow index (BFI) and is generally assumed to be proportional to the particles' velocity: $BFI = \frac{1}{K^2}$.[37,38] Calculated BFI was subsequently used to dynamically measure vessel diameter, as per previous studies.[39]

Whiskers were stimulated with 10 repetitions of the air puff cycle. Each cycle consisted of 5 s stimulation at 5 Hz and 30 s delay. Relative BFI was calculated for each cycle by dividing it with BFI averaged over 5 s preceding the stimuli.[40] A response magnitude map was calculated for each cycle and a 50×50 pixel region of interest (ROI) placed automatically around the area with the strongest response when averaged over all cycles. The relative BFI changes averaged over the ROI were then used to compare the NVC responses between groups. Mean BFI changes were calculated within this ROI over time to evaluate the amplitude of whisker stimulation responses. Four mice, one from each of the four study groups, lacked whiskers and were therefore excluded from the assessment of NVC. Other measurements of these four mice, assumed to be independent of whether the mice had whiskers, such as resting arterial diameter and arterial blood flow, were included in the analysis.

Telemetric blood pressure measurements

In a separate study, six each wild type and $\alpha_2^{+/G301R}$ mice were instrumented with pressure probes (PA-C10, Data Sciences International (DSI, USA) to measure circadian blood pressure in awake mice in their home cages. Mice were anaesthetized with isoflurane (induction: 3.5% isoflurane in 100% O_2 with a flow of 0.8 L/min; maintenance: 1.5–1.7% isoflurane in 100% O_2 and a 0.8 L/min through a mask) and the radiotelemetry catheter was inserted into the common carotid artery with the transmitter body subcutaneously. The skin incision was closed using 6-0 nonabsorbable suture and mice recovered for a week prior the measurements were started. A painkiller (0.2 mL/kg; Temgesic; Schering-Plough Europe, USA) was injected subcutaneously immediately after anaesthesia was induced and supplied to drinking water (0.01 mg/mL) for three days after surgery. The telemetric blood pressure signal was recorded at 256 Hz frequency in one-minute intervals each second minute for at least 24 hours from 6 p.m. to 6 p.m. the following day. Registration and primary analysis were performed with Ponemah 8 (DSI) software. For data presentation, the measured arterial pressure was averaged per one hour data points. For comparisons of diurnal and nocturnal blood pressures between genotypes, a blood pressure over 3 hours was averaged, i.e., over periods from 11 a.m. to 2 p.m. and from 11 p.m. to 2 a.m.

Venous blood analysis

Venous blood was analyzed and compared between genotypes under baseline conditions and after 14 days treatment with pNaKtide. Mice were briefly sedated with 2% isoflurane and the cheek pouch vein was punctured by a needle. Blood was sampled in a capillary tube and analyzed using an ABL 80 or ABL 90 device (Radiometer, Denmark).

Cerebrospinal fluid assessment

Cerebrospinal fluid (CSF) was collected from mice anesthetized with ketamine (80 mg/kg, Ketaminol vet, Intervet International, Boxmeer, Netherlands) and xylazine (10 mg/mL, Rompun® Vet). An incision was made through the skin over the neck and skeletal muscle tissue between the basis of the skull and the upper cervical bone, C1, gently dissected. Dura was punctured at the level of cisterna magna, and 15–20 µL CSF was collected in a capillary tube over approximately 15 min. The samples were stored at −80°C. The Na^+ and K^+ concentrations in the samples were measured using flame photometry (420 Flame Photometer, Sherwood, UK) where 10 µL CSF was diluted in 15 µL Milli-Q water and then diluted 200× in 3 mM LiCl in Milli-Q.

Whole-mount $K_{ir}2.1$ staining

Mice were heparinized and perfusion-fixed under 3% isoflurane anesthesia with 4% paraformaldehyde (PFA) in Dulbecco's $CaCl_2$ and $MgCl_2$-free phosphate buffered saline (PBS, in mM: 137 NaCl, 2.7 KCl, 1.5 KH_2PO_4, 8.9 Na_2HPO_4) through the left cardiac ventricle. The middle cerebral artery and downstream branches were dissected and post-fixed for 24 h in 4% PFA and afterward stored in 2% PFA in PBS at 4°C. The tissues were blocked with blocking buffer (1% bovine serum albumin and 0.2% Triton-X in PBS) for 2 h at room temperature, and washed twice and incubated with primary antibody (rabbit anti-potassium channel $K_{ir}2.1$ antibody, 1:100, #Q64273, Sigma-Aldrich, St. Louis, MO, USA) in blocking buffer overnight at 4°C. Tissues were subsequently washed and incubated with secondary antibody (donkey anti-rabbit IgG, CF™ 633 conjugate, 1:100, Sigma-Aldrich) in 0.1% Triton in PBS for 2 h at room temperature. Samples were mounted in glycerol containing 0.002% propidium iodide for nuclei visualization, and coverslipped. Samples were examined under uniform settings using confocal microscopy (FV1000 Olympus, North Ryde, Australia; excitation 637 nm/emission 650 nm; excitation 561 nm/emission 615 nm).

Statistics

Data is presented as mean ± standard deviation, n equals number of mice. Probability (P) values < 0.05 were considered statistically significant. Data processing and statistical analyses were performed using MATLAB (ver. R2022b) and GraphPad Prism software (ver. 10). The groups were compared using two-way ANOVA followed by Bonferroni post-test for multiple comparisons.

Results

Increased pial artery tone in $\alpha_2^{+/G301R}$ mice normalized after pNaKtide treatment

The diameter, blood flow, and velocity of the 3rd order branch of the middle cerebral artery was assessed in awake mice using laser speckle contrast imaging (Figure 1(a) to (c)). Artery diameter was reduced in $\alpha_2^{+/G301R}$ mice before the treatment (Figure 1(d)). The increased arterial tone in $\alpha_2^{+/G301R}$ mice before treatment was associated with reduced arterial blood flow whereas blood flow index, as proportional to velocity, was similar to that of WT mice (Figure 1(e) and (f)). *Ex vivo* cerebrovascular hypercontractility in $\alpha_2^{+/G301R}$ mice is associated with Src kinase-dependent sensitization of smooth muscle contraction to intracellular Ca^{2+}.[19] Thus, chronic inhibition of Na,K-ATPase-dependent Src kinase activation with pNaKtide was associated with a normalization of artery diameter in $\alpha_2^{+/G301R}$ mice (Figure 1(g)) whereas velocity was unchanged by the treatment (Figure 1(h)). The 14 d pNaKtide treatment increased blood flow in arteries of $\alpha_2^{+/G301R}$ mice, but not in WT (Figure 1(i)). A separate control group of WT and $\alpha_2^{+/G301R}$ mice received vehicle treatment for 14 d, which was not associated with change in artery diameter, velocity, or blood flow (Figure 1(g) to (i)).

Normalization of cerebral blood flow in $\alpha_2^{+/G301R}$ mice was not associated with arterial blood pressure changes

To assess whether differences in cerebral blood flow occurred as a result of variation in arterial blood pressure, circadian blood pressure in wild type and in $\alpha_2^{+/G301R}$ mice was recorded with radiotelemetry (Suppl. Fig. 1). No difference in heart rate, systolic, diastolic and mean arterial blood pressure was detected between genotypes. The pNaKtide treatment tended to cause minor reduction in these parameters, mostly during daytime (Suppl. Fig. 1).
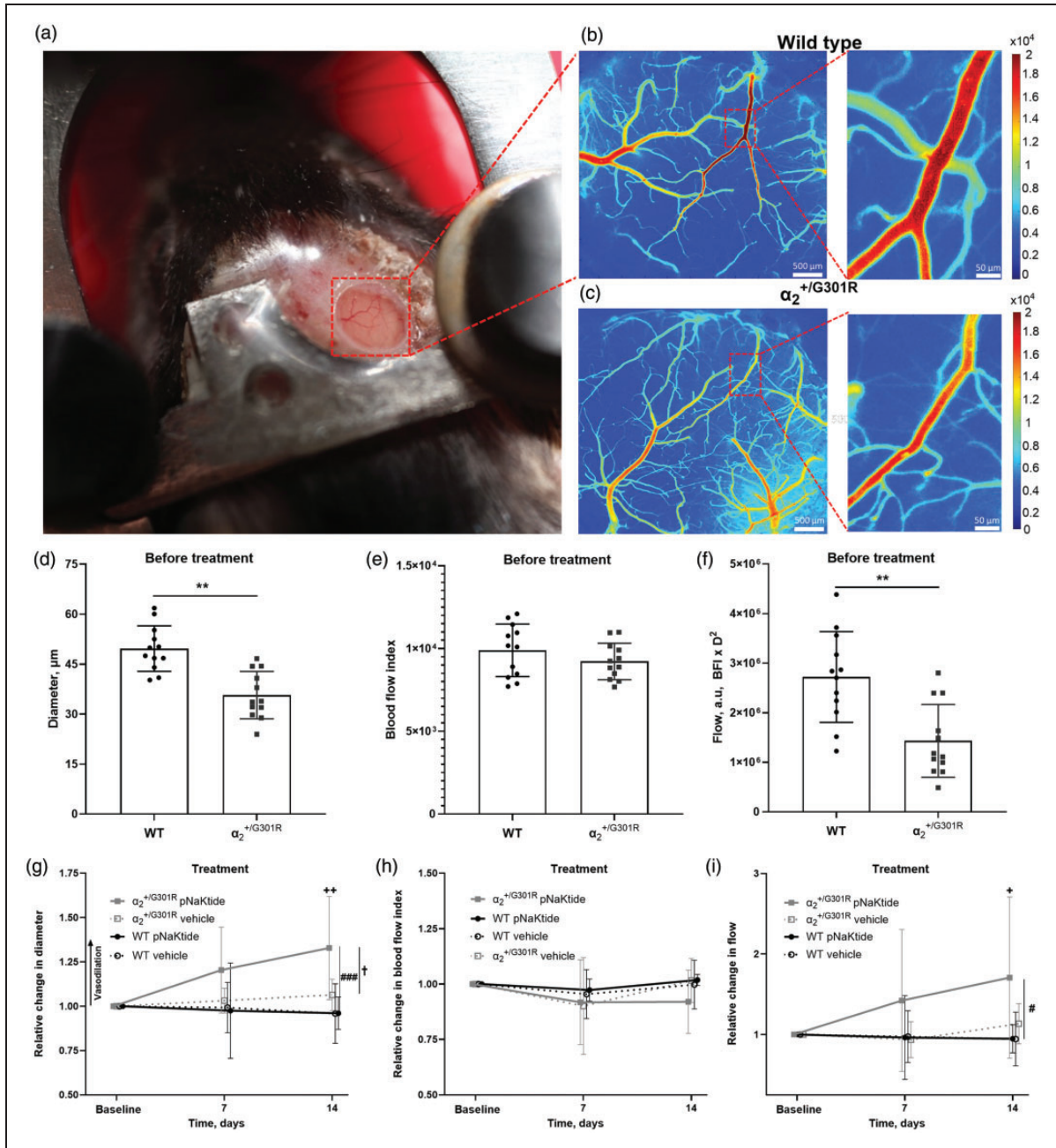
Figure 1. Increased cerebrovascular tone in $\alpha_2^{+/G301R}$ mice was prevented by pNaKtide, an inhibitor of the Na,K-ATPase-dependent Src signaling. Representative image of a head-fixed awake mouse with a chronic cranial window (a). Representative laser speckle contrast images from a wild type (WT; b) and a $\alpha_2^{+/G301R}$ mouse before treatment (c). The diameter of the 3rd order branch of the middle cerebral artery (MCA) was reduced in awake $\alpha_2^{+/G301R}$ mice prior to treatment compared with WT mice (d; $n = 12$). The MCA blood flow index (BFI), which is proportional to velocity, did not differ between genotypes (e), with reduced diameter being associated with a lower blood flow (BFI*D^2; a.u., arbitrary units) in MCAs from $\alpha_2^{+/G301R}$ mice before the treatment compared with that of WT (f). Arterial diameter was increased in $\alpha_2^{+/G301R}$ mice after 14 days pNaKtide treatment (g; $n = 6$). The pNaKtide treatment did not change arterial diameter in WT mice ($n = 6$), and vehicle-treated mice of both genotypes ($n = 6$) also showed no change in diameter over time. The velocity was not statistically different after pNaKtide treatment or vehicle treatment in any of the genotypes (h). The 14 d pNaKtide treatment increased blood flow in $\alpha_2^{+/G301R}$ mice but did not change blood flow in pNaKtide-treated WT, nor $\alpha_2^{+/G301R}$ and WT mice receiving vehicle (i). ** indicates $P < 0.01$ for comparison between genotypes before treatment; +, ++ indicate $P < 0.05$, and 0.01 for comparison of the effect of 14 d pNaKtide treatment with baseline values in $\alpha_2^{+/G301R}$ mice; #, ### indicate $P < 0.05$, 0.001, comparing $\alpha_2^{+/G301R}$ and WT mice after 14 d pNaKtide treatment; † indicates $P < 0.05$, for pNaKtide-treated compared with vehicle-treated $\alpha_2^{+/G301R}$ mice. Data, mean ± SD. Data was compared with two-way ANOVA followed by Bonferroni *post-test* for multiple comparisons.

Inhibition of the Na,K-ATPase-dependent Src kinase signaling normalized neurovascular coupling in $\alpha_2^{+/G301R}$ mice

Neurovascular coupling was assessed in awake mice using laser speckle contrast imaging (Figure 2(a)). There was no significant difference in resting blood flow index in the sensory cortex between genotypes (Suppl. Fig. 2). Relative change in blood flow in the sensory cortex was measured in response to air-puff whisker stimulation (Suppl. Video). Before the treatment, $\alpha_2^{+/G301R}$ mice showed exaggerated NVC compared with WT (Figure 2(b)). The difference in NVC between the genotypes was abolished after 7 and 14 d of treatment with pNaKtide (Figure 2(c) and (d)). Neurovascular coupling in WT mice was unaffected after 14 d of pNaKtide treatment (Suppl. Fig. 3A). In contrast, NVC was reduced in $\alpha_2^{+/G301R}$ mice after pNaKtide treatment compared with responses before treatment (Suppl. Fig. 3B). Vehicle treatment did not change NVC in any of the genotypes (Suppl. Fig. 3C,D).

Altered endothelial $K_{ir}2.1$ expression in arterioles from $\alpha_2^{+/G301R}$ mice is corrected with pNaKtide treatment

Expression of $K_{ir}2.1$ in cerebral vessels was assessed in mice treated for 14 d with either pNaKtide or vehicle.

There was no difference between genotypes in endothelial and smooth muscle cell $K_{ir}2.1$ expression in the middle cerebral or pial artery (Figure 3(a) to (f)). Similar expression levels between genotypes were observed in mice treated with vehicle, and in pNaKtide-treated mice. The vehicle-treated $\alpha_2^{+/G301R}$ mice showed an increased endothelial $K_{ir}2.1$ expression in downstream cerebral arterioles compared with WT (Figure 3(g)). This difference between genotypes was abolished after 14 d pNaKtide treatment. There was no difference in $K_{ir}2.1$ expression in arteriole smooth muscle cells between the genotypes in either of the intervention groups (Figure 3(h)).

Altered blood parameters and pNaKtide treatment

The CSF K^+ and Na^+ concentrations were similar between genotypes in vehicle-treated groups (Figure 4(a) and (b)). The 14 d pNaKtide treatment did not change the CSF K^+ or Na^+ concentration in any of the genotypes compared with mice of the corresponding genotype in the vehicle-treated groups. There were no differences between genotypes in any of the parameters in the venous blood analysis in the vehicle group (Figure 5(a) to (f)). In mice treated with pNaKtide for 14 d, there was an elevation of Na^+ and Cl^- in both genotypes compared with the mice of the same
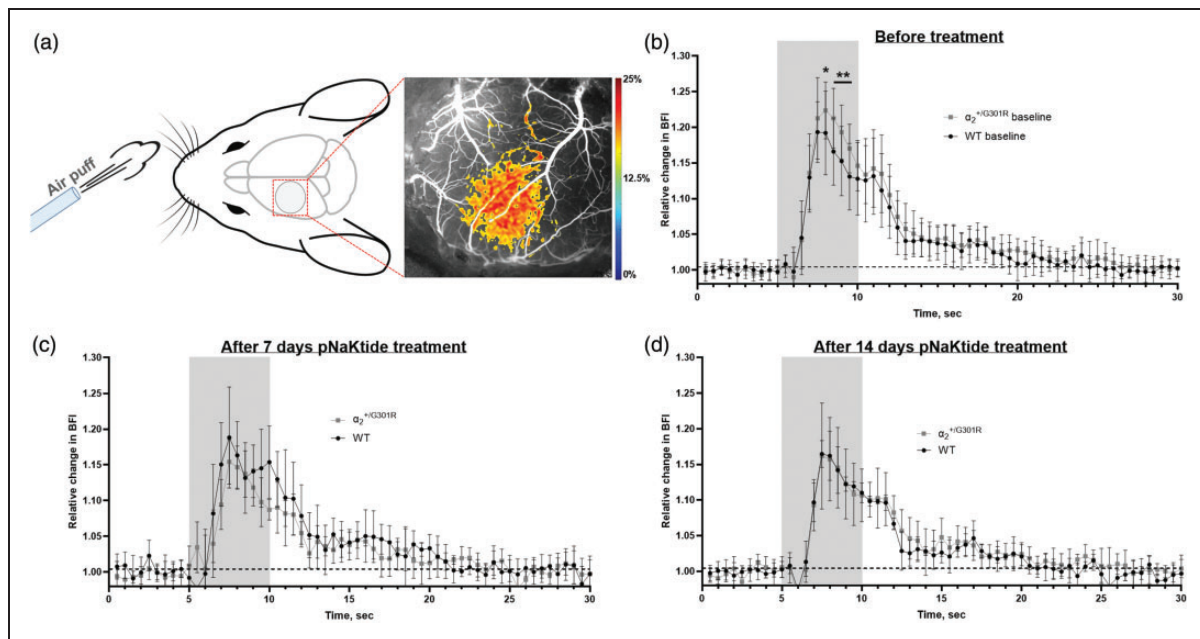

Figure 2. Chronic pNaKtide treatment normalized exaggerated neurovascular coupling responses (NVC) in the $\alpha_2^{+/G301R}$ mice. Graphical illustration of experimental setup including representative laser speckle contrast imaging showing the relative change in blood flow in the sensory cortex in response to whisker stimulation (a). Whisker stimulation is indicated in grey. The NVC response was compared at baseline before the group division into pNaKtide-treated and vehicle groups. At baseline, $\alpha_2^{+/G301R}$ mice showed an amplified NVC response compared with wild type (WT; b; $n = 10$). The difference between the groups was abolished after 7 d (c) and 14 d of pNaKtide treatment (d; $n = 5$). See also Suppl. Fig. 3 for comparison with vehicle-treated groups. Drawing of mouse head in (a) by Dr. Luigi Petrucco. Data, mean ± SD. Neurovascular coupling responses were compared between genotypes with two-way ANOVA followed with Bonferroni *post-test* for multiple comparisons; *, ** indicate $P < 0.05, 0.01$.
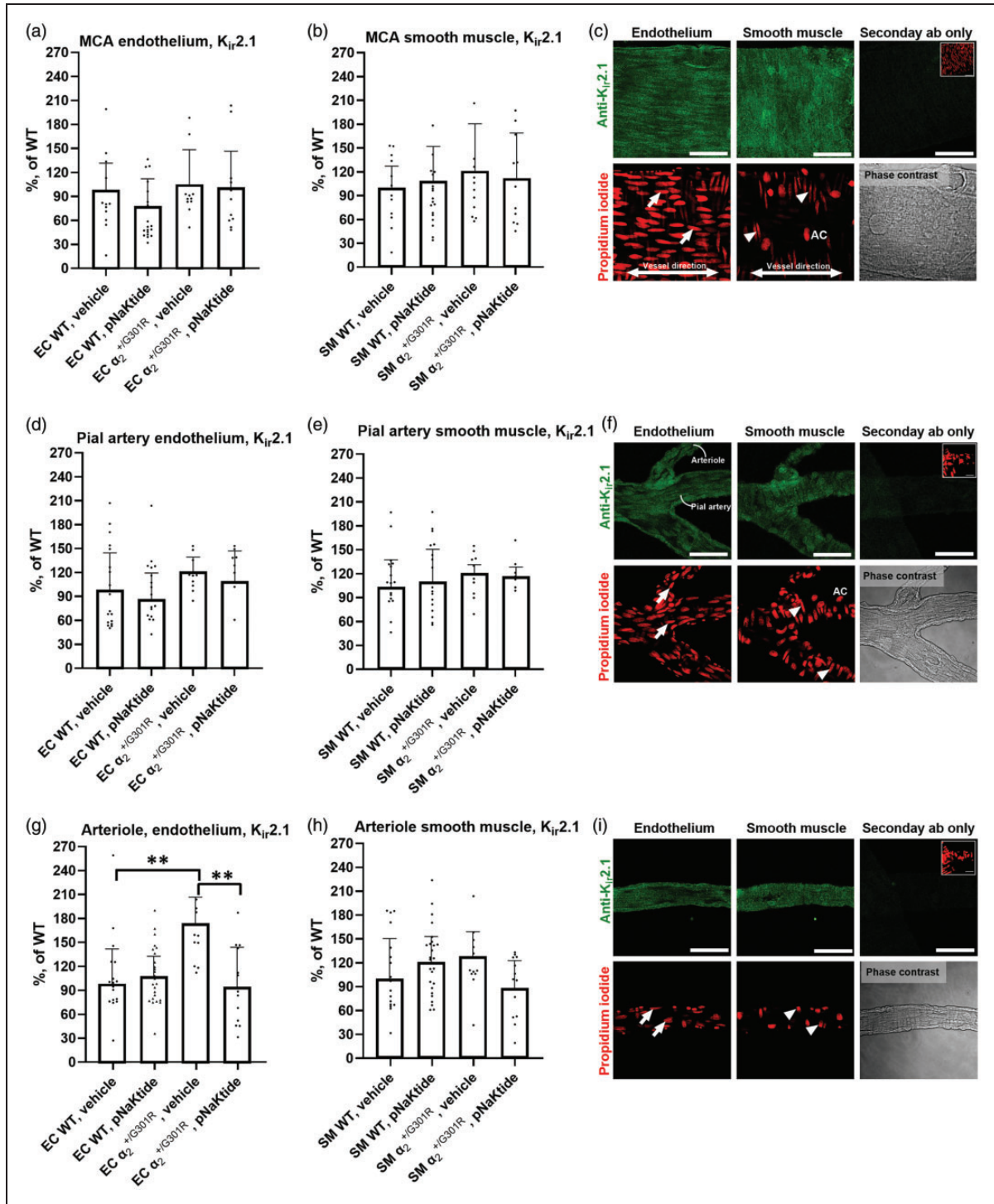
Figure 3. Increased expression of endothelial $K_{ir}2.1$ ion channels in arterioles from $\alpha_2^{+/G301R}$ compared with wild-type (WT) mice. Endothelial and SMC $K_{ir}2.1$ expression (green) in middle cerebral (MCA; a-c), downstream pial arteries (d–f), and arterioles (g–i); with EC (arrows), SMC (arrowhead), and adventitial cell (AC) propidium iodide labelled nuclei (red). Brightness was uniformly applied (c,f, i). Scale bars = 50 μm. Expression of arteriolar endothelial $K_{ir}2.1$ was increased in $\alpha_2^{+/G301R}$ mice compared with WT (g). Treatment with pNaKtide for 14 d normalized expression of arteriolar endothelial $K_{ir}2.1$ in $\alpha_2^{+/G301R}$ mice compared with pNaKtide-treated WT and $\alpha_2^{+/G301R}$ mice receiving vehicle. Weighted average (bars) expression was compared with two-way ANOVA followed with Bonferroni *post-test* for multiple comparison. Data, mean ± SD. **, $P < 0.01$. $n = 4$–7.
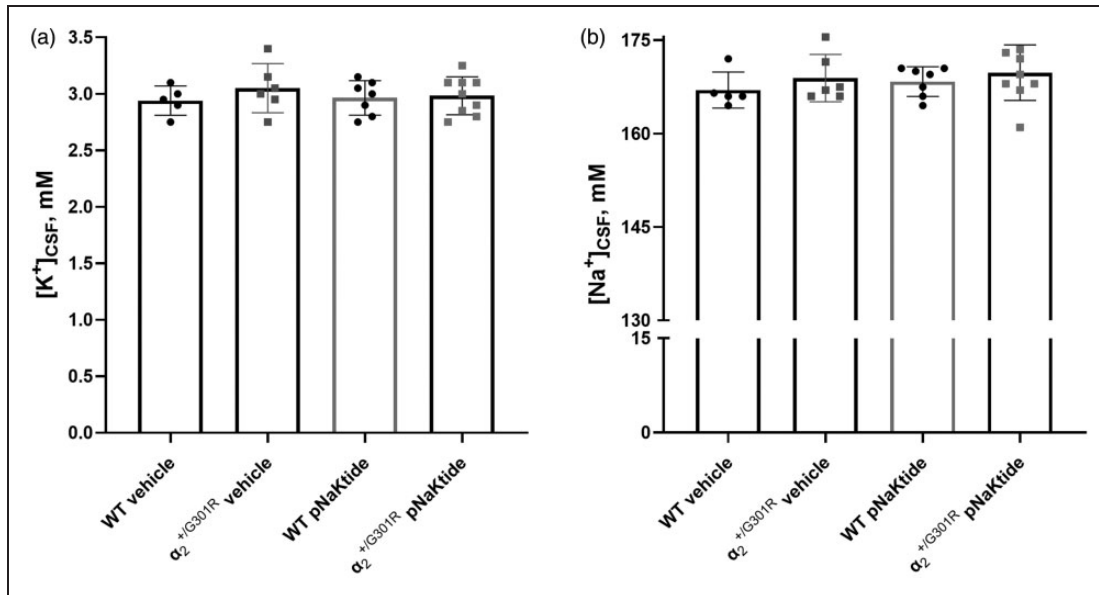
Figure 4. Sodium and potassium ion concentrations did not differ in cerebrospinal fluid (CSF) between genotypes and treatment groups. In CSF K^+ (a) and Na^+ (b) concentrations did not differ between genotypes in the vehicle-treated group, nor within each genotype when comparing pNaKtide-treated and vehicle-treated groups. Data, mean $\pm$ SD. Data were analyzed using two-way ANOVA followed by Bonferroni *post-tests* for multiple comparisons. $n = 5$–9.

genotype in the vehicle-treated group (Figure 5(b) and (e)). The concentrations of Na^+ and Cl^- were elevated in pNaKtide-treated $\alpha_2^{+/G301R}$ mice compared with pNaKtide-treated WT. In $\alpha_2^{+/G301R}$ mice, pNaKtide treatment led to a significant reduction in blood Ca^{2+}, with a similar tendency in the pNaKtide-treated WT group (Figure 5(d)). Standard bicarbonate and K^+ were elevated in pNaktide-treated WT, with a similar but not significant trend for $\alpha_2^{+/G301R}$ mice (Figure 5(c) and (f)). Blood pH was not significantly affected by the pNaKtide treatment (Figure 5(a)).

Discussion

In this study, selected cerebrovascular properties of a mouse model of FHM2 were described. Data show that $\alpha_2^{+/G301R}$ mice exhibit cerebral hypoperfusion and exaggerated NVC under baseline conditions. The aim of the study was to improve cerebral perfusion and normalize NVC in $\alpha_2^{+/G301R}$ mice with a pharmacological intervention. Previous data shows that cerebral hypoperfusion of $\alpha_2^{+/G301R}$ mice may be caused by increased Ca^{2+} sensitivity in cerebrovascular smooth muscle cells, associated with increased Na,K-ATPase-dependent Src kinase signaling.[19] By targeting this signaling with pNaKtide, the elevated cerebrovascular resistance and abnormal NVC in $\alpha_2^{+/G301R}$ mice were normalized. The results of this study provide a novel treatment target to improve cerebral blood flow in subjects carrying the FHM2-associated mutation.

Migraine with aura and cerebral hypoperfusion

Migraine with aura is associated with reduced cerebral blood flow in the interictal period.[41–43] Accordingly, the $\alpha_2^{+/G301R}$ mice show increased cerebrovascular resistance resulting in compromised cerebral blood flow. The present data show that chronic pNaKtide treatment prevented exaggerated cerebral arterial vasoconstriction in $\alpha_2^{+/G301R}$ mice *in vivo*. Previous studies showed that isolated middle cerebral arteries from $\alpha_2^{+/G301R}$ mice have exaggerated agonist-induced vasoconstriction associated with Src kinase-dependent enhanced sensitivity to intracellular Ca^{2+} in vascular smooth muscle cells.[19] Although the present study did not assess intracellular Ca^{2+} in cerebral arteries, chronic Src kinase inhibition with pNaKtide effectively reduced cerebral artery diameter of awake $\alpha_2^{+/G301R}$ mice. This result may have significant clinical implications as it suggests that targeting the Src kinase signaling *in vivo* may correct abnormal cerebral blood flow in FHM2 patients. A similar vasodilatory effect of pNaKtide may be expected in WT mice, based on observations from isolated arteries.[19,32] However, the present data suggest that the diameter of cerebral arteries of WT mice was not altered by pNaKtide treatment *in vivo*, possibly as the Na,K-ATPase-dependent Src kinase signaling does not make a significant contribution to resting cerebrovascular tone in WT mice, as suggested previously.[19]

In the present study, K^+ concentration in the CSF was not different between vehicle-treated $\alpha_2^{+/G301R}$ and
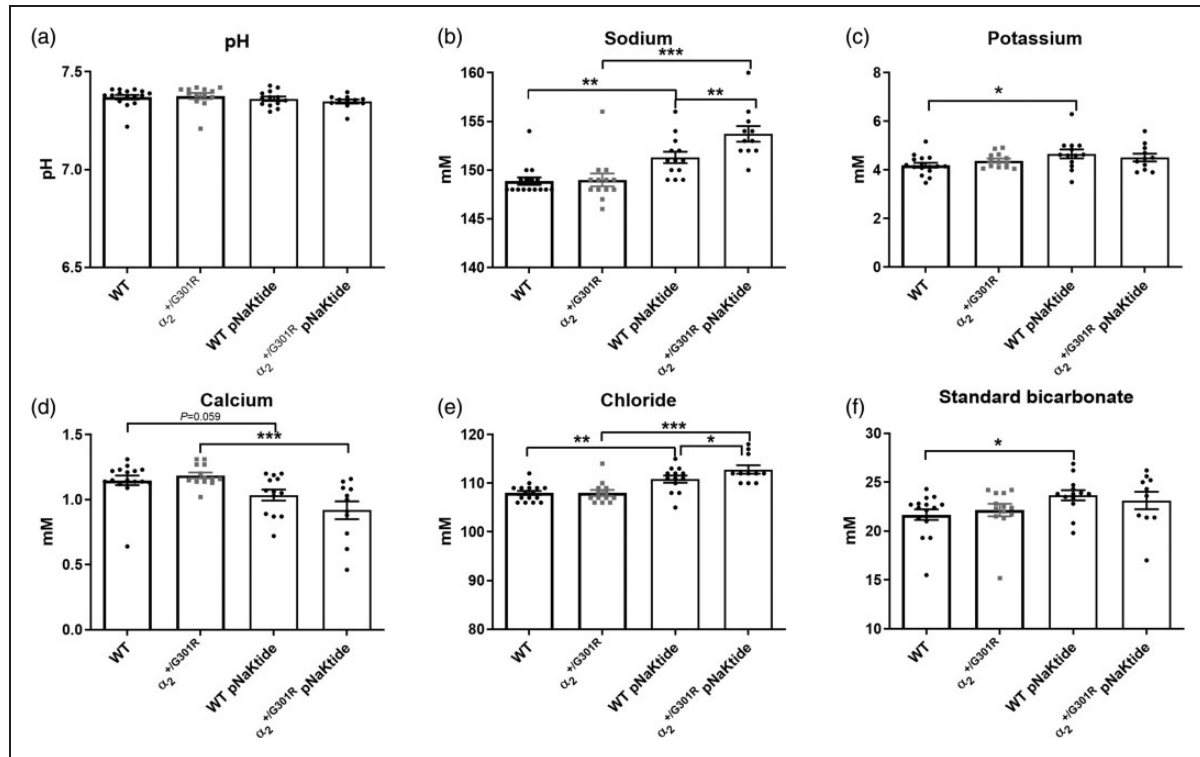
Figure 5. pNaKtide treatment changed blood parameters. Venous blood sampled from the cheek pouch was analyzed. No difference in parameters was seen between genotypes within the non-treated groups, or after 14 days of pNaKtide treatment (25 mg/kg every second day), except Na^+ (b) and Cl^- (e) concentrations, which were elevated in pNaKtide treated $\alpha_2^{+/G301R}$ mice compared with pNaKtide treated wild types. Both genotypes within the treated group showed elevated Na^+ (b) and Cl^- (e) compared with that in the corresponding non-treated group. The $\alpha_2^{+/G301R}$ mice treated with pNaKtide ($n = 11$) showed reduced Ca^{2+} (d) compared with the non-treated $\alpha_2^{+/G301R}$ mice ($n = 13$). K^+ (c) bicarbonate (f) in wild type (WT) mice treated with pNaKtide ($n = 13$) was elevated compared with non-treated WT mice ($n = 16$). Data, mean ± SD. Groups were compared using two-way ANOVA with Bonferroni's multiple comparisons test where *, **, *** indicate $P < 0.05, 0.01, 0.001$.

WT mice. This is consistent with a previous report, which suggested a similar concentration of K^+ in the parenchyma of cerebellum brain slices of $\alpha_2^{+/G301R}$ and WT mice.[18] These results suggest that the heightened susceptibility to CSD observed in previous preclinical studies[12–14,18] is more likely linked to reduced glutamate clearance than to elevated K^+ levels in the brain parenchyma in FHM2. The measured Na^+ concentrations in CSF in the present study were abnormally high, possibly because of experimental conditions, e.g., anaesthesia, although previous studies using sodium-sensitive microelectrode reported CSF Na^+ concentration of 160 mM for isoflurane-anaesthetised mice.[44] Nevertheless, the similar levels of CSF K^+ and Na^+ concentrations in both vehicle-treated mice and those treated with pNaKtide, across both genotypes, suggest that the Na,K-ATPase α_2 isoform mutation and pNaKtide treatment did not affect CSF electrolyte composition. Further clarification is warranted to determine whether restoration of cerebral blood flow with pNaKtide normalizes the previously reported

disturbance in glutamate signaling in mouse models of FHM2.[11–14]

The pNaKtide treatment resulted in increased blood Na^+, K^+ and Cl^-, and reduced Ca^{2+} concentrations. Further, standard bicarbonate levels increased in the blood in both genotypes after pNaKtide treatment, suggesting that the treatment may have caused compensatory metabolic alkalosis. These findings may result from altered renal function due to pNaKtide treatment, but further investigation is required to clarify this. Altered blood parameters are a potential adverse effect of pNaKtide at 25 mg/kg. A prior investigation has demonstrated that pNaKtide at 25 and 10 mg/kg display comparable efficacy in treating uremic cardiomyopathy in a preclinical rodent model.[29] Whether a reduced dose of pNaKtide may be efficient in restoring cerebral perfusion in subjects with the FHM2-associated mutation remains to be investigated. Additionally, it is unknown whether a lower dosage of pNaKtide will also elicit electrolyte imbalances, as observed in mice at the higher dosage.

Systemic blood pressure is an important factor defining the perfusion gradient and thus, cerebral blood flow.[45] Whether WT and $\alpha_2^{+/G301R}$ mice differ in systemic cardiovascular parameters and if pNaKtide modifies them, affecting cerebral perfusion and neurovascular coupling response, was determined. Consistent with our previous telemetry measurements in 3-month-old mice,[46] no difference in heart rate, systolic, diastolic and mean arterial blood pressure between genotypes occurred. Although increased tone occurs in cerebral arteries,[19,20] this is not a uniform observation. Thus, peripheral resistance arteries, such as small mesenteric arteries of $\alpha_2^{+/G301R}$ mice, do not show any difference in contractility compared with WT,[19] suggesting a background for similar blood pressure regulation between genotypes. Although minor reduction in blood pressure and heart rate occurred two weeks after pNaKtide treatment, this did not affect the difference between genotypes. Accordingly, the same 25 mg/kg pNaKtide treatment every second day for four weeks was previously reported to be without effect on cardiovascular parameters in sham operated and partial nephrectomized WT mice.[29] Therefore, it seems unlikely that changes in systemic cardiovascular parameters contribute to abnormal cerebrovascular function in $\alpha_2^{+/G301R}$ mice. Of note, there is no difference in blood pressure between control subjects and patients with FHM2.[47]

In the present study, whisker stimulation led to an exaggerated increase in blood flow in the sensory cortex of awake $\alpha_2^{+/G301R}$ mice compared with WT. These results are in line with previous data suggesting exaggerated NVC in anesthetized $\alpha_2^{+/G301R}$ mice.[20] Brain slice experiments suggest that abnormal NVC in $\alpha_2^{+/G301R}$ mice is caused by excessive vasodilation associated with elevated $K_{ir}2.1$ expression in the cerebrovascular endothelium.[20] Consistently, data from the present study showed that $\alpha_2^{+/G301R}$ mice have increased expression of endothelial $K_{ir}2.1$ in cerebral arterioles, whereas no difference between genotypes was observed in upstream arteries. This implies that the increased presence of endothelial $K_{ir}2.1$ in cerebral arterioles, as the primary site determining vascular resistance, enhances the vasodilation in response to increased extracellular K^+ concentration upon neuronal excitation. Another relevant factor is that elevated baseline arterial tone can influence the NVC response through several non-linear parameters, potentially enhancing the vasodilation in response to whisker stimulation. In $\alpha_2^{+/G301R}$ mice, the elevated baseline tone of cerebral arteries may contribute to amplifying the relative change in perfusion in response to whisker stimulation. In fact, the resting parenchymal blood flow index in the whisker sensory cortex tended to be reduced in $\alpha_2^{+/G301R}$ mice before the pNaKtide treatment, although the difference between genotypes did not reach significance. Thus, assessing NVC as a change in flow relative to baseline has limitations, as the flow response to neuronal activation depends on the baseline arterial tone. Consequently, the greater capacity for vasodilation in $\alpha_2^{+/G301R}$ mice, with elevated baseline arterial tone, may have contributed to the observed exaggerated NVC response. However, the previous *ex vivo* analysis on isolated middle cerebral arteries showed that the exaggerated K_{ir}-dependent vasodilation in $\alpha_2^{+/G301R}$ mice compared with WT mice is independent from the pre-constriction level,[20] arguing for increased neurovascular coupling independently from baseline perfusion. Further analysis is needed to test whether this *ex vivo* difference can be normalized with chronic pNaKtide treatment.

Previous magnetic resonance imaging studies have shown exaggerated blood oxygenation level-dependent (BOLD) signal in response to visual stimulation during the interictal period in individuals with migraine with aura.[48–51] This response may reflect exaggerated functional hyperemia that might be caused by a lower threshold for neuronal excitation in the visual cortex in migraine with aura,[52] a mechanism that might also contribute to the increased susceptibility to aura-associated CSD. However, in $\alpha_2^{+/G301R}$ mice, exaggerated neurovascular coupling responses are observed despite similar Ca^{2+} responses in neurons and astrocytes compared to WT mice in cortical brain slices.[20] This suggests that the increased potency for vasorelaxation, rather than altered neuronal excitability, may underlie the increased neurovascular coupling in this FHM2 mouse model. In light of this, the current discovery of a connection between increased arteriole endothelial $K_{ir}2.1$ expression and exaggerated NVC linked to the FHM2-associated mutation is compelling.

Notably, pNaKtide treatment not only restored normal cerebral perfusion under resting conditions in $\alpha_2^{+/G301R}$ mice, but also normalized the exaggerated NVC. These results suggest that this normalization of NVC may be because of normalization in endothelial $K_{ir}2.1$ expression. We speculate that the disturbance in NVC in $\alpha_2^{+/G301R}$ mice before pNaKtide treatment may be a consequence of endothelial $K_{ir}2.1$ upregulation as a compensatory response to cerebral hypoperfusion. Notably, exposure of cultured cerebral capillary endothelial cells to chronic low oxygen levels results in an upregulation of $K_{ir}2.1$ expression.[53] This implies that cerebral hypoperfusion in $\alpha_2^{+/G301R}$ mice, per the current study, may result in impaired oxygen availability. This chronic tissue hypoxia may increase the expression of endothelial $K_{ir}2.1$ channels in downstream arterioles leading to abnormal NVC. However, this point requires further clarification to be conclusive.

The study has several limitations. Although mice were trained and habituated for the experimental setup, the use of awake mice may cause lesser than optimal levels of stability in cerebral blood flow due to spontaneous neuronal activity and locomotion,[54] which was not corrected for. However, a significant strength of the study is its avoidance of anesthesia, thereby preventing the challenges of it suppressing neuronal activity and systemic and cerebral vasodilation, which greatly impact NVC.[55,56] Another limitation is that the laser speckle imaging system was not calibrated to specific flow, which hindered the quantification of such flow in absolute values. However, maintaining constant laser speckle parameters and ensuring a speckle size exceeding 2 pixels enables comparisons of blood flow measures in arbitrary units.[35,57,58] Finally, the $\alpha_2^{+/G301R}$ mouse model, which carries a mutation associated with a severe phenotype in humans,[10] may not fully reflect the cerebrovascular and neuronal phenotypes in human subjects carrying this or other FHM2-associated mutations, or more common types of migraine with aura.

Conclusion

The results of the present study suggest that targeting Na,K-ATPase-dependent Src kinase activation prevents cerebral hypoperfusion and disturbance in NVC in a mouse model of FHM2. Data suggest a novel treatment target to restore normal cerebral blood flow in FHM2. Future studies will clarify whether normalization of cerebral blood flow with pNaKtide reduces the susceptibility to CSD in subjects carrying the FHM2-associated mutation.

Data availability statement

All study data are available from the corresponding author upon reasonable request.

Declaration of conflicting interests

The author(s) declared no potential conflicts of interest with respect to the research, authorship, and/or publication of this article.

Authors' contributions

CS and VVM conceived and designed the study. CS, HOG, and CH conducted the experiments. CS, HOG, CH, DP, and SLS performed the data analysis. DP, SP, and SLS contributed to the methodology. CS wrote the initial draft of the manuscript, and all authors reviewed, edited, and approved the final version. CS and VVM secured funding for the study.

Supplementary material

Supplemental material for this article is available online.

ORCID iDs

Christian Staehr https://orcid.org/0000-0001-5431-4409
Tina M Pedersen https://orcid.org/0000-0001-7950-4647
Vladimir V Matchkov https://orcid.org/0000-0002-3303-1095

References

1. Isaksen TJ and Lykke-Hartmann K. Insights into the pathology of the α2-Na(+)/K(+)-ATPase in neurological disorders; lessons from animal models. *Front Physiol* 2016; 7: 161–20160504.
2. Friedrich T, Tavraz NN and Junghans C. ATP1A2 mutations in migraine: Seeing through the facets of an ion pump onto the neurobiology of disease. *Front Physiol* 2016; 7: 239–20160621.
3. De Fusco M, Marconi R, Silvestri L, et al. Haploinsufficiency of ATP1A2 encoding the Na+/K+ pump alpha2 subunit associated with familial hemiplegic migraine type 2. *Nat Genet* 2003; 33: 192–196.
4. Larsen BR, Assentoft M, Cotrina ML, et al. Contributions of the Na$^+$/K$^+$-ATPase, NKCC1, and Kir4.1 to hippocampal K$^+$ clearance and volume responses. *Glia* 2014; 62: 608–622.
5. Conti F and Pietrobon D. Astrocytic glutamate transporters and migraine. *Neurochem Res* 2023; 48: 1167–1179.
6. Cholet N, Pellerin L, Magistretti PJ, et al. Similar perisynaptic glial localization for the Na+,K+-ATPase α2 subunit and the glutamate transporters GLAST and GLT-1 in the rat somatosensory cortex. *Cereb Cortex* 2002; 12: 515–525.
7. Staehr C, Rajanathan R and Matchkov VV. Involvement of the Na+,K+-ATPase isoforms in control of cerebral perfusion. *Exp Physiol* 2019; 104: 1023–1028.
8. Matchkov VV and Krivoi II. Specialized functional diversity and interactions of the Na,K-ATPase. *Front Physiol* 2016; 7: 179.
9. Staehr C, Aalkjaer C and Matchkov VV. The vascular Na,K-ATPase: clinical implications in stroke, migraine, and hypertension. *Clin Sci (Lond)* 2023; 137: 1595–1618.
10. Spadaro M, Ursu S, Lehmann-Horn F, et al. A G301R Na+/K+ -ATPase mutation causes familial hemiplegic migraine type 2 with cerebellar signs. *Neurogenetics* 2004; 5: 177–185.
11. Bøttger P, Glerup S, Gesslein B, et al. Glutamate-system defects behind psychiatric manifestations in a familial

hemiplegic migraine type 2 disease-mutation mouse model. *Sci Rep* 2016; 6: 22047.

12. Leo L, Gherardini L, Barone V, et al. Increased susceptibility to cortical spreading depression in the mouse model of familial hemiplegic migraine type 2. *PLOS Genet* 2011; 7: e1002129.

13. Parker PD, Suryavanshi P, Melone M, et al. Non-canonical glutamate signaling in a genetic model of migraine with aura. *Neuron* 2021; 109: 611–628.e8.

14. Capuani C, Melone M, Tottene A, et al. Defective glutamate and K+ clearance by cortical astrocytes in familial hemiplegic migraine type 2. *EMBO Mol Med* 2016; 8: 967–986.

15. Stoica A, Larsen BR, Assentoft M, et al. The α2β2 isoform combination dominates the astrocytic Na(+)/K(+) -ATPase activity and is rendered nonfunctional by the α2.G301R familial hemiplegic migraine type 2-associated mutation. *Glia* 2017; 65: 1777–1793.

16. Cozzolino O, Marchese M, Trovato F, et al. Understanding spreading depression from headache to sudden unexpected death. *Front Neurol* 2018; 9: 19–20180201.

17. Erdener ŞE, Kaya Z and Dalkara T. Parenchymal neuroinflammatory signaling and dural neurogenic inflammation in migraine. *J Headache Pain* 2021; 22: 138–20211118.

18. Kros L, Lykke-Hartmann K and Khodakhah K. Increased susceptibility to cortical spreading depression and epileptiform activity in a mouse model for FHM2. *Sci Rep* 2018; 8: 16959–11.

19. Staehr C, Hangaard L, Bouzinova EV, et al. Smooth muscle Ca(2+) sensitization causes hypercontractility of middle cerebral arteries in mice bearing the familial hemiplegic migraine type 2 associated mutation. *J Cereb Blood Flow Metab* 2019; 39: 1570–1587.

20. Staehr C, Rajanathan R, Postnov DD, et al. Abnormal neurovascular coupling as a cause of excess cerebral vasodilation in familial migraine. *Cardiovasc Res* 2020; 116: 2009–2020.

21. Nedeltchev K, Arnold M, Schwerzmann M, et al. Cerebrovascular response to repetitive visual stimulation in interictal migraine with aura. *Cephalalgia* 2004; 24: 700–706.

22. Thie A, Carvajal-Lizano M, Schlichting U, et al. Multimodal tests of cerebrovascular reactivity in migraine: a transcranial doppler study. *J Neurol* 1992; 239: 338–342.

23. Longden TA, Dabertrand F, Koide M, et al. Capillary K(+)-sensing initiates retrograde hyperpolarization to increase local cerebral blood flow. *Nat Neurosci* 2017; 20: 717–726.

24. Harraz OF, Longden TA, Dabertrand F, et al. Endothelial GqPCR activity controls capillary electrical signaling and brain blood flow through PIP(2) depletion. *Proc Natl Acad Sci U S A* 2018; 115: E3569–e3577.

25. Dabertrand F, Harraz OF, Koide M, et al. PIP(2) corrects cerebral blood flow deficits in small vessel disease by rescuing capillary Kir2.1 activity. *Proc Natl Acad Sci U S A* 2021; 118: e2025998118.

26. Longden TA, Dabertrand F, Hill-Eubanks DC, et al. Stress-induced glucocorticoid signaling remodels neurovascular coupling through impairment of cerebrovascular inwardly rectifying K+ channel function. *Proc Natl Acad Sci U S A* 2014; 111: 7462–7467.

27. Longden TA and Nelson MT. Vascular inward rectifier K+ channels as external K+ sensors in the control of cerebral blood flow. *Microcirculation* 2015; 22: 183–196.

28. Sancho M, Fabris S, Hald BO, et al. Membrane Lipid-K(IR)2.x channel interactions enable hemodynamic sensing in cerebral arteries. *Arterioscler Thromb Vasc Biol* 2019; 39: 1072–1087.

29. Liu J, Tian J, Chaudhry M, et al. Attenuation of Na/K-ATPase mediated oxidant amplification with pNaKtide ameliorates experimental uremic cardiomyopathy. *Sci Rep* 2016; 6: 34592–2016.

30. Hangaard L, Bouzinova EV, Staehr C, et al. Na-K-ATPase regulates intercellular communication in the vascular wall via cSrc kinase-dependent connexin43 phosphorylation. *Am J Physiol Cell Physiol* 2017; 312: C385–c397.

31. Kutz LC, Cui X, Xie JX, et al. The Na/K-ATPase α1/src interaction regulates metabolic reserve and Western diet intolerance. *Acta Physiol (Oxf)* 2021; 232: e13652.

32. Bouzinova EV, Hangaard L, Staehr C, et al. The α2 isoform Na,K-ATPase modulates contraction of rat mesenteric small artery via cSrc-dependent Ca(2+) sensitization. *Acta Physiol (Oxf)* 2018; 224: e13059.

33. Rognant S, Kravtsova VV, Bouzinova EV, et al. The microtubule network enables src kinase interaction with the Na,K-ATPase to generate Ca(2+) flashes in smooth muscle cells. *Front Physiol* 2022; 13: 1007340–20220923.

34. Li Z, Cai T, Tian J, et al. NaKtide, a Na/K-ATPase-derived peptide src inhibitor, antagonizes ouabain-activated signal transduction in cultured cells. *J Biol Chem* 2009; 284: 21066–21076.

35. Postnov DD, Cheng X, Erdener SE, et al. Choosing a laser for laser speckle contrast imaging. *Sci Rep* 2019; 9: 2542–20190222.

36. Akther S, Mikkelsen MB and Postnov DD. Choosing a polarisation configuration for dynamic light scattering and laser speckle contrast imaging. *Biomed Opt Express* 2024; 15: 336–345.

37. Liu C, Kılıç K, Erdener SE, et al. Choosing a model for laser speckle contrast imaging. *Biomed Opt Express* 2021; 12: 3571–3583.

38. Dunn AK, Bolay H, Moskowitz MA, et al. Dynamic imaging of cerebral blood flow using laser speckle. *J Cereb Blood Flow Metab* 2001; 21: 195–201.

39. Postnov DD, Tuchin VV and Sosnovtseva O. Estimation of vessel diameter and blood flow dynamics from laser speckle images. *Biomed Opt Express* 2016; 7: 2759–2768.

40. Staehr C, Giblin JT, Gutiérrez-Jiménez E, et al. Neurovascular uncoupling is linked to microcirculatory dysfunction in regions outside the ischemic core following ischemic stroke. *J Am Heart Assoc* 2023; 12: e029527.

41. Facco E, Munari M, Baratto F, et al. Regional cerebral blood flow (rCBF) in migraine during the interictal

period: different rCBF patterns in patients with and without aura. *Cephalalgia* 1996; 16: 161–168.

42. Calandre EP, Bembibre J, Arnedo ML, et al. Cognitive disturbances and regional cerebral blood flow abnormalities in migraine patients: their relationship with the clinical manifestations of the illness. *Cephalalgia* 2002; 22: 291–302.

43. Nowaczewska M, Straburzyński M, Waliszewska-Prosół M, et al. Cerebral blood flow and other predictors of responsiveness to erenumab and fremanezumab in migraine – a real-life study. *Front Neurol* 2022; 13: 895476–20220517.

44. Van Huysse JW, Amin MS, Yang B, et al. Salt-induced hypertension in a mouse model of liddle syndrome is mediated by epithelial sodium channels in the brain. *Hypertension* 2012; 60: 691–696. 20120716.

45. Cipolla MJ. *Integrated systems physiology: from molecule to function. The cerebral circulation*. San Rafael, CA: Morgan & Claypool Life Sciences. Copyright © 2010 by Morgan & Claypool Life Sciences, 2009.

46. Staehr C, Rohde PD, Krarup NT, et al. Migraine-associated mutation in the Na,K-ATPase leads to disturbances in cardiac metabolism and reduced cardiac function. *J Am Heart Assoc* 2022; 11: e021814.

47. Hansen JM, Thomsen LL, Marconi R, et al. Familial hemiplegic migraine type 2 does not share hypersensitivity to nitric oxide with common types of migraine. *Cephalalgia* 2008; 28: 367–375.

48. Datta R, Aguirre GK, Hu S, et al. Interictal cortical hyperresponsiveness in migraine is directly related to the presence of aura. *Cephalalgia* 2013; 33: 365–374.

49. Vincent M, Pedra E, Mourão-Miranda J, et al. Enhanced interictal responsiveness of the migraineous visual cortex to incongruent bar stimulation: a functional MRI visual activation study. *Cephalalgia* 2003; 23: 860–868.

50. Fabjan A, Zaletel M and Žvan B. Is there a persistent dysfunction of neurovascular coupling in migraine? *BioMed Res Int* 2015; 2015: 574186.

51. Griebe M, Flux F, Wolf ME, et al. Multimodal assessment of optokinetic visual stimulation response in migraine with aura. *Headache: J Head Face Pain* 2014; 54: 131–141.

52. Battelli L, Black KR and Wray SH. Transcranial magnetic stimulation of visual area V5 in migraine. *Neurology* 2002; 58: 1066–1069.

53. Yamamura H, Suzuki Y, Yamamura H, et al. Hypoxic stress upregulates Kir2.1 expression by a pathway including hypoxic-inducible factor-1alpha and dynamin2 in brain capillary endothelial cells. *Am J Physiol Cell Physiol* 2018; 315: C202–C213.

54. Eyre B, Shaw K, Sharp P, et al. The effects of locomotion on sensory-evoked haemodynamic responses in the cortex of awake mice. *Sci Rep* 2022; 12: 6236–04.

55. Gao Y-R, Ma Y, Zhang Q, et al. Time to wake up: studying neurovascular coupling and brain-wide circuit function in the un-anesthetized animal. *NeuroImage* 2017; 153: 382–398.

56. Franceschini MA, Radhakrishnan H, Thakur K, et al. The effect of different anesthetics on neurovascular coupling. *Neuroimage* 2010; 51: 1367–1377. 2010/03/31.

57. Kirkpatrick SJ, Duncan DD and Wells-Gray EM. Detrimental effects of speckle-pixel size matching in laser speckle contrast imaging. *Opt Lett* 2008; 33: 2886–2888.

58. Boas DA and Dunn AK. Laser speckle contrast imaging in biomedical optics. *J Biomed Opt* 2010; 15: 011109.